Host-directed therapy with 2-Deoxy-D-glucose inhibits human rhinoviruses, endemic coronaviruses, and SARS-CoV-2

Laxmikant Wali[1,5], Michael Karbiener[2,5], Scharon Chou[1], Vitalii Kovtunyk[1], Adam Adonyi[1], Irene Gösler[3], Ximena Contreras[1], Delyana Stoeva[1], Dieter Blaas[3], Johannes Stöckl[4], Thomas R. Kreil[2], Guido A. Gualdoni[1] and Anna-Dorothea Gorki[1,6]

[1] G.ST Antivirals GmbH, Austria

[2] Global Pathogen Safety, Takeda Manufacturing Austria AG , Austria

[3] Center of Medical Biochemistry, Max Perutz Labs, Vienna Biocenter, Medical University of Vienna, Austria

[4] Institute of Immunology, Center of Pathophysiology, Immunology & Infectiology, Medical University of Vienna, Austria

[5] Contributed equally

[6] Corresponding author

Abstract word count: 122

Text word count: 3470

Figures: 5 Main Figures

Corresponding Author:
Anna-Dorothea Gorki, PhD,
G.ST Antivirals GmbH,
Doktor-Bohr-Gasse 7 (VBC6) 1030 Vienna, Austria
Phone: +43 6641869461
E-mail: anna-dorothea.gorki@gst-antivirals.com

KEYWORDS: antiviral, broad-spectrum antiviral therapy, 2-DG, rhinovirus, coronavirus, SARS-CoV-2

HIGHLIGHTS

- 2-DG, a glucose analogue, inhibits RV RNA replication and reduces RV-mediated cell death *in vitro*.
- 2-DG exhibits increased inhibitory activity against RV in physiological glucose concentrations *in vitro*.
- 2-DG attenuates viral load of pandemic and endemic CoVs *in vitro*.

ABSTRACT

Rhinoviruses (RVs) and coronaviruses (CoVs) upregulate host cell metabolic pathways including glycolysis to meet their bioenergetic demands for rapid multiplication. Using the glycolysis inhibitor 2-deoxy-D-glucose (2-DG), we confirm the dose-dependent inhibition of minor- and major-receptor group RV replication. We demonstrate that 2-DG suppresses viral positive- as well as negative-strand RNA synthesis, resulting in lower amounts of progeny virus and RV-mediated cell death. In tissue culture with physiologic glucose levels, 2-DG has a pronounced antiviral effect. Further, assessment of 2-DG´s intracellular kinetics revealed that the active intermediate, 2-DG6P, is stored intracellularly for several hours. Our concurrent study of 2-DG´s impact on pandemic SARS-CoV-2 and endemic HCoVs demonstrated a significant reduction in viral load. Collectively, these results suggest 2-DG to be a broad-spectrum antiviral.

INTRODUCTION

Rhinoviruses (RVs) and endemic coronaviruses (HCoVs) are the major cause of acute respiratory tract (RT) infections in humans [1], [2]. These are largely self-limiting in healthy adults, where they usually remain confined to the upper respiratory tract. However, as the viruses spread rapidly and circulate seasonally, they lead to high incidence rates on an annual basis. These can cause severe morbidity in

elderly, children, and immune-compromised patients [3]–[6]. Along with human suffering, these viral infections lead to high economic losses and healthcare costs [7], [8]. While global efforts are underway to develop an effective therapy, the current lack of FDA-approved antivirals has limited the treatment of RT infections to supportive and symptomatic care.

As *Picornaviridae*, RVs are non-enveloped and contain a positive-sense single-stranded RNA genome ((+)ssRNA) [9]. They are divided into three species, RV-A, RV-B and RV-C. RV-A and RV-B are further classified as minor- and major-group based on the cognate host cell receptors they use for cell entry [10]–[12]. Coronaviruses (CoVs) are enveloped viruses, belong to the *Coronaviridae* family and contain a (+)ssRNA genome as well [13]. They are classified into four major genera: alpha, beta, gamma, and delta, targeting a variety of host species. In humans, strains from the alpha [14]–[16] and beta genera [17] are known to induce common colds similar to the ones caused by RVs [18], [19]. However, three strains from the beta genus, including Severe Acute Respiratory Syndrome Coronavirus 2 (SARS-CoV-2) were found to be more pathogenic with high fatality rates [20].

Viruses are dependent on the host cell metabolism and host cell machinery to ensure their replication. RVs and CoVs in particular are known to hijack and reprogram the host cell metabolic pathways for rapid multiplication, causing an increase in bioenergetic demand [21], [22]. This leads to an elevated anabolic state, forcing the host cell to synthesize more lipids and nucleotides using glucose and glutamine as substrates [23]. In addition, there is an increased demand for energy in the form of adenosine triphosphate (ATP) for viral replication and assembly, which is predominantly provided by glycolysis [23]–[25]. As an essential metabolic pathway, this involves breakdown of hexoses like glucose into pyruvate for ATP production. This dependency of RVs and CoVs, and presumably other viruses on host glucose metabolism for replication presents a promising target for the development of effective antiviral therapies.

2-Deoxy-D-glucose (2-DG), a stable analogue of glucose, is taken up by cells via glucose transporters and subsequently phosphorylated to 2-deoxy-D-glucose-6-phosphate (2-DG6P) by hexokinase [26], [27]. Unlike in glucose metabolism, 2-DG6P

cannot be further metabolized by phosphoglucose isomerase [28]. This leads to intracellular accumulation of 2-DG6P and arrest of glycolysis at the initial stage, causing depletion of glucose derivatives and substrates crucial for viral replication [29]. Previously, it has been demonstrated that 2-DG affects viral replication by reverting virus-induced metabolic reprogramming of host cells [24], [25], [30], [31].

In the present study, we investigated the antiviral activity of 2-DG against minor- and major-group RVs in epithelial cells including primary human nasal epithelial cells, the main site of RV replication. Concomitantly, we explored the effect of glucose on the antiviral activity of 2-DG and characterized 2-DG´s intracellular kinetics. To better understand the inhibitory activity of 2-DG on the RV replication cycle, we quantified both the (+)ssRNA as well as the template (-)ssRNA strand. In addition, we analyzed the 2-DG's effect on RV-mediated cell death. Finally, we assessed the antiviral activity of 2-DG against endemic CoVs as well as the pandemic SARS-CoV-2 strain. Reverting virus-induced metabolic reprogramming by 2-DG treatment critically affected viral RNA replication and thus holds great potential in combating respiratory viral infections.

METHODS

Details of all materials used are listed in Supplement Table 1.

Cell culture. Cells were seeded in 24-well tissue culture plates and incubated at 37 °C in media and densities (cells per well) for the given times as indicated below; human nasal epithelial cells (HNECs) in HNEC medium at $4.5x10^4$ (72 h) and HeLa Ohio cells in HeLa Ohio medium at $2x10^5$ (16-20 h). LLC-MK2 and MRC-5 cells were cultured in T25 cell culture flasks in the corresponding media at densities of $8x10^5$ and $9x10^5$, respectively. The details of the culture medium and supplements used are listed in Supplement Table 1.

Viral infection and 2-DG treatment. HeLa Ohio cells and HNECs were infected for 1 h at 37 °C or 34 °C with RV at 0.005 to 0.5 $TCID_{50}$/cell and $4.5x10^4$ $TCID_{50}$/well, followed by treatment with 2-DG for 6 h, 24 h or 48 h. The supernatant from the cells were then subjected to virus titer analysis or, the cells were treated with cell lysis buffer for RNA extraction. LLC-MK2 cells and MRC-5 cells were infected with SARS-CoV-2 (Beta-CoV/Germany/BavPat1/2020) (MOI of 0.001) at 36 °C and HCoV-229E (MOI of 0.01) at 36 °C or HCoV-NL63 (MOI of 0.01) at 33 °C, respectively. Cells were treated with 2-DG 1 h post-infection and samples were collected at the indicated times for virus titer analysis.

RNA isolation and cDNA synthesis. Intra- and extra-cellular RNA was isolated according to the ExtractMe Total RNA Kit instructions. To avoid bias in extracellular RNA isolation, an internal spike-in RNA control was added to each sample. RNA concentration and purity was assessed using a nanophotometer. cDNA was synthesized according to the First strand cDNA synthesis kit using the program: 37 °C for 60 min and 70 °C for 5 min. Measurement of viral negative strand RNA ((-)RNA) was performed as previously described [32] except that the synthesized cDNA wasn't RNase treated and purified. The cDNA from (-)RNA was synthesized using a mix of strand-specific, chimeric sequences-containing primer chimHRV-b14_RT and control primer HPRT_R (Supplement Table 1) instead of oligo(dT).

qPCR. qPCR was performed using SYBR green mix and primers as described in Supplement Table 1. For measuring intracellular viral RNA, gene expression was normalized to HPRT using the Livak method [33] and expressed as fold change to control (infected, but untreated). Primers HRV-B14_R and chimHRV-b14_R1 were used for measurement of viral (-)RNA. For extracellular viral RNA, synthetic oligo standard (HRV-B14_F, HRV-B14_R and HRV-B14 primer amplicon, Supplement Table 1) were used to generate a standard curve for the calculation of viral copy number by interpolation. Based on the qPCR data, the IC_{50} was calculated using least square regression on Prism 9.0.2.

Virus titration. Samples from SARS-CoV-2, HCoV-229E and HCoV-NL63 were titrated on Vero cells, MRC-5 cells, and LLC-MK2 cells, respectively. Samples from RV-B14 were titrated on HeLa Ohio cells. Titration was performed using eightfold replicates of serial half-log_{10} (for SARS-CoV-2, HCoV-229E and HCoV-NL63) or log_{10} (for RV-B14) dilutions of virus-containing samples followed by incubation at 36 °C (SARS-CoV-2, HCoV-229E), 33 °C (HCoV-NL63) and 34 °C (RV-B14) for 5-7 days (SARS-CoV-2, HCoV-229E, RV-B14) or 9-11 days (HCoV-NL63). Wells were inspected under a microscope for cytopathic effect (CPE). For RV-B14, CPE was visualized by crystal violet staining. Recognizable CPE at each tested dilution was used to determine the dose according to Reed and Muench [34] and reported as log_{10}-transformed median tissue culture infectious dose per milliliter (log_{10}[$TCID_{50}$/mL]).

Virus-induced cytopathic effect. HeLa Ohio cells were infected for 1 h at 37 °C with RV-B14 (0.5 $TCID_{50}$/cell) followed by 2-DG treatment for 24 h or 48 h at 37 °C. CPE was visualized by crystal violet staining. The effect of 2-DG on virus-induced cell death was assessed by calculating the ratio of the average of treated, uninfected to each treated, infected sample value.

Crystal violet staining. Cells were incubated with crystal violet solution (0.05% crystal violet in 20% methanol) for 30-60 min, washed with ddH_2O, air-dried, followed by 25% glacial acetic acid. The absorbance was recorded at 450nm.

Glucose-uptake assay. Cells were treated with 2-DG in the absence of glucose for 10 min at 37 °C, followed by washing with PBS and incubation for up to 270 min in glucose-free medium. 2-DG uptake was assessed using the Glucose-Uptake Glo™ Assay kit. Luminescence was recorded on a microplate reader. 2-DG6P levels were calculated as percentage of signal upon exposure to 2-DG after subtracting the background value obtained from control samples (not treated with 2-DG).

Statistical analysis. The graphs show pooled results of independent experiments with each experiment containing two to four cell culture wells per condition with the standard error of the mean (SEM). Analysis of statistical significance was performed using Student´s *t*-test (unpaired analysis) or 2-way-ANOVA with Bonferroni´s correction and considered significant when $p < 0.05$ (*$p \leq 0.05$, **$p \leq 0.01$, ***$p \leq 0.001$, ****$p \leq 0.0001$).

RESULTS

2-DG inhibits RV replication in HeLa Ohio cells and HNECs

2-Deoxyglucose (2-DG) treatment has been shown to inhibit rhinovirus (RV) infection by reverting RV-induced anabolic reprogramming of host cell metabolism [25]. First, we determined whether similar results [25] could be observed not only for RV-B14, used in the above-mentioned study, but also for additional RV stains from the minor-group (RV-A1B, RV-A2) and the major-group (RV-A89, RV-A16, RV-A54). HeLa Ohio cells were infected under conventional culture conditions using a medium containing 2 g/L glucose. We found that 2-DG treatment led to a dose-dependent reduction in intracellular viral RNA levels of all major- and minor-group RVs tested (Figure 1A). The highest tested concentration of 2-DG (30 mM) showed a reduction in intracellular viral RNA of up to 96.1 % ± 2.9 % (mean ± SEM) in RV-B14 (Figure 1A). These results are consistent with the previous study in which 2-DG inhibited RV-B14 replication in HeLa cells and in primary human fibroblasts [25]. We then evaluated the effect of 2-DG on RV-B14 and RV-A16 replication in human nasal epithelial cells (HNECs), the natural replication site for rhinoviruses. In line with the previous findings, 10 mM and 30 mM 2-DG treatment strongly inhibited RV-B14 and RV-A16 replication (Figure 1B). To be noted, unlike in HeLa Ohio cell culture medium, where the glucose level is known, glucose levels in HNECs culture medium are not disclosed by the manufacturer. Together, the data suggests that 2-DG inhibits RV replication in a dose-dependent manner, independent of the viral strain and cell type used.

Inhibitory activity of 2-DG is dependent on glucose level

2-DG, a glucose analogue, is transported into cells utilizing the same transporters as glucose, resulting in a competition for the uptake of 2-DG [26], [27]. The glucose concentration in conventional cell culture media ranges from 2 g/L to 4.5 g/L. This is much higher than *in vivo* glucose levels (e.g., in the blood, which is in the range of 3.9 to 5.6 mmol/L i.e., 0.7 to 1 g/L). To understand the uptake and activity of 2-DG at physiological glucose levels, we reduced the glucose concentration in the cell culture medium to 1 g/L to mimic a setting corresponding to human plasma. As in the conventional cell culture setup above (Figure 1), HeLa Ohio cells were separately

infected with six different RV strains. Again, we observed that 2-DG suppressed RV replication in a dose-dependent manner, with 30 mM 2-DG leading to complete abolishment of RV replication (Figure 2A). In addition, 3 mM and 10 mM 2-DG caused a pronounced reduction in intracellular viral RNA for all tested RV strains (Figure 2A). In line with these results, the absolute half-maximal inhibitory concentration (IC_{50}) of 2-DG was lower under physiological glucose conditions (Figure 2B, Supplementary Table 2). The IC_{50} ranged from 1.92 mM to 2.67 mM as compared to 3.44 mM to 9.22 mM for cells infected and treated under conventional culture conditions (i.e., in the presence of 2 g/L glucose). These results indicate better uptake and enhanced activity of 2-DG at physiological glucose levels.

A short exposure to 2-DG leads to extended intracellular storage of 2-DG6P

Once 2-DG is taken up by the cell, it is phosphorylated to 2-deoxy-D-glucose-6-phosphate (2-DG6P), which leads to the arrest of glycolysis and altering of viral replication [25]. Thus, the kinetics of cellular uptake and intracellular storage are crucial for the antiviral activity of 2-DG. Therefore, we investigated the intracellular concentration kinetics of 2-DG6P in HeLa Ohio cells and HNECs. Cells were treated with 1 mM and 10 mM 2-DG, respectively, for 10 min. At time zero (immediately after the 10 min 2-DG treatment), higher 2-DG6P levels were observed in 10 mM 2-DG treatment compared to 1 mM 2-DG treatment, in both HeLa Ohio cells and HNECs (Figure 3A, 3B, left graph). The intracellular 2-DG6P level measured at time zero was then set to 100 %, and the percentage decay of 2-DG6P over time was calculated. In HeLa Ohio cells 3.5 % ± 0.6 % (mean±SEM) and 18.5 % ± 3.4 % 2-DG6P were measured in 1 mM and 10 mM 2-DG treated cells after 270 min (Figure 3A). In the case of HNECs, higher levels of 2-DG6P retention were observed after 270min; 10.1% ± 1.5% and 42.6 % ± 7.2 % 2-DG6P being detected in 1 mM and 10 mM 2-DG treated cells (Figure 3B), respectively. Collectively, the data suggest that short exposure of the cells to 2-DG leads to an intracellular accumulation of the active intermediate 2-DG6P for several hours.

2-DG disrupts RNA template strand synthesis and inhibits RV-mediated cell death

After confirming that 2-DG strongly suppresses RV replication and has a pronounced effect at physiological glucose conditions, we further investigated which step of the RV replication cycle was targeted. First, we analyzed the influence of 2-DG on synthesis of (-)ssRNA and of (+)ssRNA, 24h post-infection. Consistent with the above findings of intracellular virus levels after 7 h post-infection (Figure 2A), 10 mM 2-DG treatment led to a significant decrease in (+)ssRNA levels of RV-B14 at 24 h post-infection (Figure 4A). This result was closely mirrored by decrease in the (-)ssRNA template strand upon 2-DG treatment (Figure 4A). Simultaneously, we found that 2-DG treatment led to a significant decrease in the number of viral RNA copies in the supernatant (Figure 4B), implying an impairment of the amount of released virus. Next, we assessed 2-DG´s impact on viral load by means of median tissue culture infectious dose ($TCID_{50}$) assays. RV-B14 infected HeLa Ohio cells were treated with 2-DG at 3.57 mM, corresponding to IC_{90}, up to 48 h and the supernatants containing progeny virus were collected every 24 h and analyzed. The above IC_{90} concentration of 2-DG was calculated from the previously derived dose-response curve in HeLa Ohio cells (Figure 2A, RV-B14). In comparison to the untreated cells, 2-DG treated cells showed a clear reduction in viral load 48 h post-infection (Figure 4C).

A characteristic of RV infection of tissue culture cells is the cytopathic effect (CPE) [35]. The impact of increasing concentrations of 2-DG on RV-induced cell death was assessed in HeLa Ohio cells at 24 h and 48 h post-infection. A significant protective effect was seen in cells treated with 2-DG at 1 mM or higher after 24 h (Figure 4D). At 48 h post-infection, the CPE was stronger in untreated cells (‘Virus only’) but, again, cell death was significantly reduced upon treatment with 2-DG at 0.33 mM or higher (Figure 4D). Together, these results suggest that 2-DG affects the RV life cycle by suppressing viral RNA replication and viral load and reduces RV-mediated cell death.

2-DG decreases CoV viral load

Similar to RVs, SARS-CoV-2 was recently shown to exploit the host glucose metabolism for replication and can potentially be targeted by 2-DG [24], [35]. With this rationale we investigated the effect of 2-DG on the viral load of the pandemic strain, SARS-CoV-2, as well as the two endemic human CoV stains, HCoV-229E and HCoV-NL63. Cells with known susceptibility to these coronaviruses were treated with

293 increasing doses of 2-DG for 24 h to 48 h. The supernatant containing released virus
294 was sampled every 24 h and viral load was assessed as $TCID_{50}$. We observed a
295 significant reduction in SARS-CoV-2 at 24 h post-infection at the highest tested 2-DG
296 concentration (10 mM), and further, lower 2-DG concentrations led to significant
297 effects 48h post-infection (Figure 5A). A similar behavior was observed for HCoV-
298 229E, where 24 h and 48 h post-infection a significant reduction in viral load was
299 observed in cells treated with 0.32 mM and 1 mM 2-DG (Figure 5B). The use of lower
300 2-DG concentrations was based on decreased viability of MRC5 cells at 2-DG
301 concentrations above 1 mM (data not shown). In the case of HCoV-NL63, there was
302 no significant decrease in viral load at 24 h, however, at 48 h post-infection 2-DG
303 concentrations above 1 mM suppressed viral load significantly (Figure 5C). These
304 results suggest that 2-DG exerts a dose-dependent reduction in viral load of
305 pandemic as well as endemic CoV strains.
306

DISCUSSION

In this study we investigated a host-directed approach to combat rhinovirus (RV) and coronavirus (CoV) infection by using 2-Deoxy-D-glucose (2-DG). This approach is based on the understanding that virus-induced metabolic reprogramming of the host cell plays a crucial role in viral replication [21], [22], [25]. Previously, Gualdoni et al., [25] demonstrated that 2-DG reverts RV-induced metabolic reprogramming of host cells and inhibits RV-B14 replication. Consequently, in the present study, we sought to further elucidate the implications of 2-DG on the RV replication cycle, the intracellular kinetics of 2-DG and its impact on CoV viral load. We found that 2-DG treatment led to a marked inhibition of positive strand as well as negative strand RNA replication. 2-DG treatment caused a significant reduction in the extracellular viral RNA level and RV viral load as well as in the RV-mediated cytopathic effect. At a physiological glucose concentration, 2-DG treatment led to enhanced inhibition of RV replication as compared to conventional high-glucose culture conditions. Assessment of 2-DG´s intracellular kinetics showed accumulation of the active intermediate, 2-DG6P, for several hours. Our concurrent study of 2-DG´s impact on CoVs also showed a significant reduction in viral load. Taken together, the results suggest 2-DG to be a broad-spectrum antiviral.

In our study, treatment with 2-DG inhibited replication of all tested minor- and major-receptor group strains of RV in HeLa Ohio cells under conventional culture condition (i.e., 2 g/L glucose) and in primary human nasal epithelial cells (HNECs) (Figure 1). As 2-DG competes with glucose for cellular uptake [26], [27], we lowered the glucose concentration to 1 g/L glucose – mimicking the human plasma glucose concentration – to assess the efficacy of 2-DG in a physiological context. We found that lower glucose concentrations potentiated 2-DG-mediated inhibition of RV replication, pointing to a higher efficacy of 2-DG in physiological settings (Figure 2, Supplement Table 2). It should be noted that the glucose concentration in fluid lining the nose and lung epithelium in humans is around 12.5 times lower than in plasma [36]. Therefore, it can be anticipated that 2-DG exhibits even higher antiviral efficacy in therapeutic target tissues. However, additional studies in models closer to the physiologic conditions are warranted to test this hypothesis.

In the next step, we characterized the intracellular kinetics of 2-DG. In the cell, 2-DG is phosphorylated to 2-DG6P, leading to its intracellular accumulation. Cytochalasin B, an inhibitor of the glucose transporter, was used as a control to ensure 2-DG6P specificity in our set-up (data not shown). Overall, we found that 2-DG6P was detectable up to several hours in HeLa Ohio cells and HNEC after a short incubation of the cells with 2-DG.

During the RV replication cycle, the viral polyprotein is first generated via translation from the (+)ssRNA genome, which is then processed by viral proteases to generate viral proteins including the viral RNA polymerase [37]. Next, RNA polymerase generates (-)RNA strand copies, which in turn serve as a template for the multifold replication of the positive stand viral genome to be packaged in viral capsids, finally leading to release of the mature virions [38]. As conventional RT-PCR holds limitations to detect the negative strand in excess of positive strand copies, we employed a recently published strategy by Wiehler and Proud [32] to analyze the negative strand level. We observed that 2-DG significantly reduced the genomic (+)ssRNA as well as the template (-)ssRNA, a likely cause for the measured significant reduction in detectable extracellular viral RNA (Figure 4A&B). These findings point at a 2-DG-mediated impairment in viral RNA replication and amount of released virus. In line with this, titration of the released virus on HeLa Ohio cells showed a reduction in viral load (Figure 4C). To be noted, HeLa Ohio cells used in this experimental setup, due to their cancerous origin, have a high glucose demand and are especially sensitive to glucose starvation and 2-DG treatment. Therefore, low amounts of 2-DG were used, and the cells were treated only once after the start of the RV infection. This could explain the relatively small difference in viral load (Figure 4C) in contrast to the significant difference in released extracellular viral RNA (Figure 4B).

In our subsequent analysis, we found that 2-DG exerted a protective effect by significantly reducing virus-induced cell death in HeLa Ohio cells (Figure 4D). In contrast, RV infection does not cause cell lysis in cultures of healthy bronchial epithelial cells [39]. Interestingly, the same study reported increased viral replication and cell lysis after RV infection in asthmatic bronchial epithelial cells [39]. Based on

these findings, we could envision protection of RV-infected bronchial epithelial cells from asthma patients by 2-DG.

The host metabolic dependency of CoVs is similar to that of RVs and studies suggest that 2-DG alters SARS-CoV-2 replication [24], [26], [40]. This prompted us to further investigate the effect of 2-DG on CoV viral load. In our study, 2-DG treatment of endemic and pandemic CoVs resulted in a dose-dependent reduction of viral load. Compared to our data from RV viral load, lower concentrations of 2-DG are sufficient to cause a long-term significant reduction in viral load in both endemic and pandemic CoVs. This difference between RV and CoV can be attributed to differences in cell culture models. Another possible explanation is that CoVs are enveloped [13] and contain glycosylated envelope proteins responsible for host cell interaction and infection. Along with CoVs dependence on host glucose metabolism for replication [24], they are dependent on the host cell machinery for glycosylation of viral proteins [41]. Thus, the reduction in CoV viral load could originate from 2-DG not only inhibiting glycolysis but also affecting protein and lipid glycosylation [42]. However, further studies are required to decipher a possible role of 2-DG in the production of defective virions in enveloped viruses.

In conclusion, we present a host-directed approach to tackle RV and CoV infections. The dependency of these viruses on the host cell metabolism and cell machinery reveals a therapeutic opportunity to target them with glucose analogues, such as 2-DG.

ACKNOWLEDGMENTS

We thank Melanie Graf and the Global Pathogen Safety Team (Takeda), most notably Jasmin de Silva, Elisabeth List and Effie Oindo (experiments), Veronika Sulzer (cell culture), Eva Ha, Simone Knotzer and Alexandra Schlapschy-Danzinger (virus propagation). SARS-CoV-2 was sourced via EVAg (supported by the European Community) and kindly provided by Christian Drosten and Victor Corman (Charité Universitätsmedizin, Institute of Virology, Berlin, Germany). HCoV-NL63 was kindly provided by Lia van der Hoek (Medical Microbiology, Academisch Medisch Centrum, Amsterdam, Netherlands).

FUNDING

This study was supported by a FFG Basisprogramm, grant number 36734898 (to G.ST Antivirals).

CONFLICT OF INTERESTS

L.W., S.C., V.K., A.A., X.C., D.S., A.-D.G., J.S. and G.G. are/were employees and/or shareholders of G.ST Antivirals, Vienna, Austria. G.G. and J.S. are co-inventors of patent application related to parts of the manuscript. M.K. and T.R.K. are employees and stockholders of Takeda Manufacturing Austria AG, Vienna, Austria.

AUTHOR CONTRIBUTION

L.W., M.K., S.C., V.K., A.A., X.C., D.S. and A.-D.G. performed experiments and analyzed data. D.B. and I.G. provided virus strains, reagents, and valuable input. A.-D.G., J.S., T.R.K., M.K. and G.G. were in charge of planning and directing the study. L.W and A.-D.G. wrote the manuscript with input from co-authors. All authors read and approved the final manuscript.

FIGURE LEGENDS

Figure 1: Inhibition of RV replication by 2-DG in HeLa Ohio cells and HNECs. Intracellular viral RNA was measured 7 h post-infection at 0.005 $TCID_{50}$/cell for the indicated RV strains in Hela Ohio cells (A) and in undifferentiated HNECs (infected with $4.5x10^4$ $TCID_{50}$/well) (B). Cells were treated with the indicated concentrations of 2-DG (represented on a log10 scale) 1 h post-infection until the samples were collected. Graphs show pooled results ± SEM of 3-4 independent experiments. HNEC: human nasal epithelial cells, RV: rhinovirus.

Figure 2: Inhibition of RV replication by 2-DG is dependent on the glucose level. Intracellular viral RNA was measured 7 h post-infection at 0.005 $TCID_{50}$/cell for the indicated RV strains in Hela Ohio cells in medium containing 1g/L glucose (A). Cells were treated with the indicated concentrations of 2-DG (represented on a log10 scale) 1 h post-infection until samples were collected. Comparison of IC_{50} of 2-DG on the indicated RV strains under physiological versus conventional culture conditions (B). Graphs show pooled result ± SEM of 3-4 independent experiments. RV: rhinovirus.

Figure 3: Intracellular storage of 2-DG6P after short-term exposure to 2-DG. Luminescence measurements of intracellular 2-DG6P at the indicated times after Hela Ohio cells (A) or undifferentiated human nasal epithelial cells (B) were exposed to 2-DG for 10 min. In (A) and (B), the left graphs show the 2-DG6P levels (in RLU) at time 0 min (i.e., immediately after 10 min 2-DG treatment), and the right graphs show percentage decay of 2-DG6P over time in HeLa Ohio and HNECs, respectively. Data show pooled result ± SEM of 2-3 independent experiments. RLU: relative luminescence units, HNEC: human nasal epithelial cells.

Figure 4: 2-DG disrupts RNA template strand synthesis and inhibits RV-mediated cell death. Hela Ohio cells were infected with RV-B14 (0.5 $TCID_{50}$/cell) and treated with 10 mM 2-DG for 24 h to measure intracellular positive and negative viral RNA strand (A) or released extracellular viral RNA (B). Cells infected with RV-B14 (0.005 $TCID_{50}$/cell) were treated with 3.57 mM 2-DG (IC_{90} for RV-B14) for up to

48 h at 34°C to measure viral load (C). Cells infected with RV-B14 (0.5 $TCID_{50}$/cell) and treated with the indicated concentrations of 2-DG for 24 h or 48 h at 37 °C for measurement of virus-induced cytopathic effect (D). Graphs show pooled results ± SEM of 2-4 independent experiments (A,B,D) or one experiment (C). ns: non-significant; $p < 0.05$ (*$p \leq 0.05$, **$p \leq 0.01$, ***$p \leq 0.001$, ****$p \leq 0.0001$). RV: rhinovirus.

Figure 5: 2-DG shows a dose-dependent antiviral effect on different human coronaviruses. Viral load was measured from cell culture supernatants 24 h to 48 h post-infection. 2-DG treatment with the indicated concentrations was started 1 h post-infection. Viral load of SARS-CoV-2 (BetaCoV/Germany/BavPat1/2020) (MOI 0.001) released from LLC-MK2 cells (A), HCoV-229E (MOI 0.01) released from MRC5 cells (B) and HCoV-NL-63 (MOI 0.01) released from LLC-MK2 cells (C). Graphs show pooled results ± SEM of 3 independent experiments. ns: non-significant; $p < 0.05$ (*$p \leq 0.05$, **$p \leq 0.01$, ***$p \leq 0.001$, ****$p \leq 0.0001$). SARS-CoV-2: severe acute respiratory syndrome coronavirus 2, HCoV: human corona virus.

SUPPLEMENTARY MATERIALS

Supplement Table 1: Materials used in the study.

Supplement Table 2: IC50 values of tested RV strains in Hela Ohio and HNECs.

REFERENCES

[1] H. A. Rotbart and F. G. Hayden, “Picornavirus infections: a primer for the practitioner,” *Archives of Family Medicine*, vol. 9, pp. 913–920, Mar. 2000, doi: 10.1001/archfami.9.9.913.

[2] T. K. Cabeça, C. Granato, and N. Bellei, “Epidemiological and clinical features of human coronavirus infections among different subsets of patients,” *Influenza and Other Respiratory Viruses*, vol. 7, pp. 1040–1047, Mar. 2013, doi: 10.1111/irv.12101.

[3] K. K. W. To *et al.*, “Pulmonary and extrapulmonary complications of human rhinovirus infection in critically ill patients,” *Journal of Clinical Virology: The Official Publication of the Pan American Society for Clinical Virology*, vol. 77, pp. 85–91, Mar. 2016, doi: 10.1016/j.jcv.2016.02.014.

[4] S. Lee, S. S. Chiu, P. J. S. Malik, K. Chan, H. W. Wong, and Y. Lau, “Is respiratory viral infection really an important trigger of asthma exacerbations in children?,” *European Journal of Pediatrics*, vol. 170, pp. 1317–1324, Mar. 2011, doi: 10.1007/s00431-011-1446-1.

[5] I. Hung *et al.*, “Unexpectedly Higher Morbidity and Mortality of Hospitalized Elderly Patients Associated with Rhinovirus Compared with Influenza Virus Respiratory Tract Infection,” *International Journal of Molecular Sciences*, vol. 18, p. 259, Mar. 2017, doi: 10.3390/ijms18020259.

[6] D. Santesmasses *et al.*, “COVID-19 is an emergent disease of aging,” *Aging Cell*, vol. 19, Mar. 2020, doi: 10.1111/acel.13230.

[7] D. M. Cutler and L. H. Summers, “The COVID-19 Pandemic and the 16 Trillion Virus,” *JAMA*, vol. 324, Mar. 2020, doi: 10.1001/jama.2020.19759.

[8] A. M. Fendrick, A. S. Monto, B. Nightengale, and M. Sarnes, “The Economic Burden of Non–Influenza-Related Viral Respiratory Tract Infection in the United States,” *Archives of Internal Medicine*, vol. 163, p. 487, Mar. 2003, doi: 10.1001/archinte.163.4.487.

[9] A. C. Palmenberg *et al.*, “Sequencing and Analyses of All Known Human Rhinovirus Genomes Reveal Structure and Evolution,” *Science (1979)*, vol. 324, pp. 55–59, Mar. 2009, doi: 10.1126/science.1165557.

[10] F. Hofer *et al.*, “Members of the low density lipoprotein receptor family mediate cell entry of a minor-group common cold virus.,” *Proceedings of the National Academy of Sciences*, vol. 91, pp. 1839–1842, Mar. 1994, doi: 10.1073/pnas.91.5.1839.

[11] B. A. Schuler *et al.*, “Major and minor group rhinoviruses elicit differential signaling and cytokine responses as a function of receptor-mediated signal transduction,” *PloS One*, vol. 9, p. e93897, 2014, doi: 10.1371/journal.pone.0093897.

[12] D. Blaas and R. Fuchs, “Mechanism of human rhinovirus infections,” *Molecular and Cellular Pediatrics*, vol. 3, Mar. 2016, doi: 10.1186/s40348-016-0049-3.

[13] P. C. Y. Woo, Y. Huang, S. K. P. Lau, and K.-Y. Yuen, “Coronavirus Genomics and Bioinformatics Analysis,” *Viruses*, vol. 2, pp. 1804–1820, Mar. 2010, doi: 10.3390/v2081803.

[14] L. van der Hoek *et al.*, “Identification of a new human coronavirus,” *Nature Medicine*, vol. 10, pp. 368–373, Mar. 2004, doi: 10.1038/nm1024.

[15] K. McIntosh, J. H. Dees, W. B. Becker, A. Z. Kapikian, and R. M. Chanock, “Recovery in tracheal organ cultures of novel viruses from patients with respiratory disease.,” *Proc Natl Acad Sci U S A*, vol. 57, pp. 933–940, Mar.

1967, [Online]. Available: https://www.ncbi.nlm.nih.gov/pmc/articles/PMC224637/

[16] D. Hamre and J. J. Procknow, “A New Virus Isolated from the Human Respiratory Tract.,” *Experimental Biology and Medicine*, vol. 121, pp. 190–193, Mar. 1966, doi: 10.3181/00379727-121-30734.

[17] L. Vijgen *et al.*, “Circulation of genetically distinct contemporary human coronavirus OC43 strains,” *Virology*, vol. 337, pp. 85–92, Mar. 2005, doi: 10.1016/j.virol.2005.04.010.

[18] J. O. Hendley, H. B. Fishburne, and J. M. Gwaltney, “Coronavirus infections in working adults. Eight-year study with 229 E and OC 43,” *The American Review of Respiratory Disease*, vol. 105, pp. 805–811, Mar. 1972, doi: 10.1164/arrd.1972.105.5.805.

[19] A. F. Bradburne, M. L. Bynoe, and D. A. Tyrrell, “Effects of a ‘new’ human respiratory virus in volunteers.,” *British Medical Journal*, vol. 3, pp. 767–769, Mar. 1967, [Online]. Available: https://www.ncbi.nlm.nih.gov/pmc/articles/PMC1843247/

[20] N. Kaur, R. Singh, Z. Dar, R. K. Bijarnia, N. Dhingra, and T. Kaur, “Genetic comparison among various coronavirus strains for the identification of potential vaccine targets of SARS-CoV2,” *Infection, Genetics and Evolution*, p. 104490, Mar. 2020, doi: 10.1016/j.meegid.2020.104490.

[21] E. L. Sanchez and M. Lagunoff, “Viral activation of cellular metabolism,” *Virology*, vol. 479–480, pp. 609–618, Mar. 2015, doi: 10.1016/j.virol.2015.02.038.

[22] K. A. Mayer, J. Stöckl, G. J. Zlabinger, and G. A. Gualdoni, “Hijacking the Supplies: Metabolism as a Novel Facet of Virus-Host Interaction,” *Frontiers in Immunology*, vol. 10, Mar. 2019, doi: 10.3389/fimmu.2019.01533.

[23] S. K. Thaker, J. Ch’ng, and H. R. Christofk, “Viral hijacking of cellular metabolism,” *BMC Biology*, vol. 17, Mar. 2019, doi: 10.1186/s12915-019-0678-9.

[24] A. C. Codo *et al.*, “Elevated Glucose Levels Favor SARS-CoV-2 Infection and Monocyte Response through a HIF-1α/Glycolysis-Dependent Axis,” *Cell Metabolism*, vol. 32, pp. 437–446.e5, Mar. 2020, doi: 10.1016/j.cmet.2020.07.007.

[25] G. A. Gualdoni *et al.*, “Rhinovirus induces an anabolic reprogramming in host cell metabolism essential for viral replication,” *Proceedings of the National Academy of Sciences*, vol. 115, pp. E7158–E7165, Mar. 2018, doi: 10.1073/pnas.1800525115.

[26] P. Bissonnette, H. Gagne, A. Blais, and A. Berteloot, “2-Deoxyglucose transport and metabolism in Caco-2 cells,” *American Journal of Physiology-Gastrointestinal and Liver Physiology*, vol. 270, pp. G153–G162, Mar. 1996, doi: 10.1152/ajpgi.1996.270.1.g153.

[27] A. Waki *et al.*, “The importance of glucose transport activity as the rate-limiting step of 2-deoxyglucose uptake in tumor cells in vitro,” *Nuclear Medicine and Biology*, vol. 25, pp. 593–597, Mar. 1998, doi: 10.1016/s0969-8051(98)00038-9.

[28] F. Bost, A.-G. Decoux-Poullot, J. F. Tanti, and S. Clavel, “Energy disruptors: rising stars in anticancer therapy?,” *Oncogenesis*, vol. 5, p. e188, Mar. 2016, doi: 10.1038/oncsis.2015.46.

[29] H. T. Kang and E. S. Hwang, “2-Deoxyglucose: An anticancer and antiviral therapeutic, but not any more a low glucose mimetic,” *Life Sciences*, vol. 78, pp. 1392–1399, Mar. 2006, doi: 10.1016/j.lfs.2005.07.001.

[30] K. D. Passalacqua *et al.*, “Glycolysis Is an Intrinsic Factor for Optimal Replication of a Norovirus,” *mBio*, vol. 10, Mar. 2019, doi: 10.1128/mbio.02175-18.

[31] K. A. Fontaine, E. L. Sanchez, R. Camarda, and M. Lagunoff, “Dengue Virus Induces and Requires Glycolysis for Optimal Replication,” *Journal of Virology*, vol. 89, pp. 2358–2366, Mar. 2014, doi: 10.1128/jvi.02309-14.

[32] S. Wiehler and D. Proud, “Specific Assay of Negative Strand Template to Quantify Intracellular Levels of Rhinovirus Double-Stranded RNA,” *Methods and Protocols*, vol. 4, p. 13, Mar. 2021, doi: 10.3390/mps4010013.

[33] K. J. Livak and T. D. Schmittgen, “Analysis of Relative Gene Expression Data Using Real-Time Quantitative PCR and the 2−ΔΔCT Method,” *Methods*, vol. 25, no. 4, pp. 402–408, Dec. 2001, doi: 10.1006/meth.2001.1262.

[34] L. J. REED and H. MUENCH, “A SIMPLE METHOD OF ESTIMATING FIFTY PER CENT ENDPOINTS12,” *American Journal of Epidemiology*, vol. 27, no. 3, pp. 493–497, May 1938, doi: 10.1093/oxfordjournals.aje.a118408.

[35] L. Deszcz, E. Gaudernak, E. Kuechler, and J. Seipelt, “Apoptotic events induced by human rhinovirus infection,” *Journal of General Virology*, vol. 86, pp. 1379–1389, Mar. 2005, doi: 10.1099/vir.0.80754-0.

[36] J. P. Garnett, E. H. Baker, and D. L. Baines, “Sweet talk: insights into the nature and importance of glucose transport in lung epithelium,” *European Respiratory Journal*, vol. 40, pp. 1269–1276, Mar. 2012, doi: 10.1183/09031936.00052612.

[37] S. Nirwan and R. Kakkar, “Rhinovirus RNA Polymerase,” *Viral Polymerases*, pp. 301–331, 2019, doi: 10.1016/B978-0-12-815422-9.00011-5.

[38] L. van der Linden, K. C. Wolthers, and F. J. M. van Kuppeveld, “Replication and Inhibitors of Enteroviruses and Parechoviruses,” *Viruses*, vol. 7, pp. 4529–4562, Mar. 2015, doi: 10.3390/v7082832.

[39] P. A. B. Wark *et al.*, “Asthmatic bronchial epithelial cells have a deficient innate immune response to infection with rhinovirus,” *The Journal of Experimental Medicine*, vol. 201, pp. 937–947, Mar. 2005, doi: 10.1084/jem.20041901.

[40] D. Bojkova *et al.*, “Proteomics of SARS-CoV-2-infected host cells reveals therapy targets,” *Nature*, Mar. 2020, doi: 10.1038/s41586-020-2332-7.

[41] Y. Watanabe, T. A. Bowden, I. A. Wilson, and M. Crispin, “Exploitation of glycosylation in enveloped virus pathobiology,” *Biochimica et Biophysica Acta (BBA) - General Subjects*, vol. 1863, pp. 1480–1497, Mar. 2019, doi: 10.1016/j.bbagen.2019.05.012.

[42] A. N. Bhatt *et al.*, “Glycolytic inhibitor 2-deoxy-d-glucose attenuates SARS-CoV-2 multiplication in host cells and weakens the infective potential of progeny virions,” *Life Sciences*, vol. 295, p. 120411, Mar. 2022, doi: 10.1016/j.lfs.2022.120411.

Figure 1

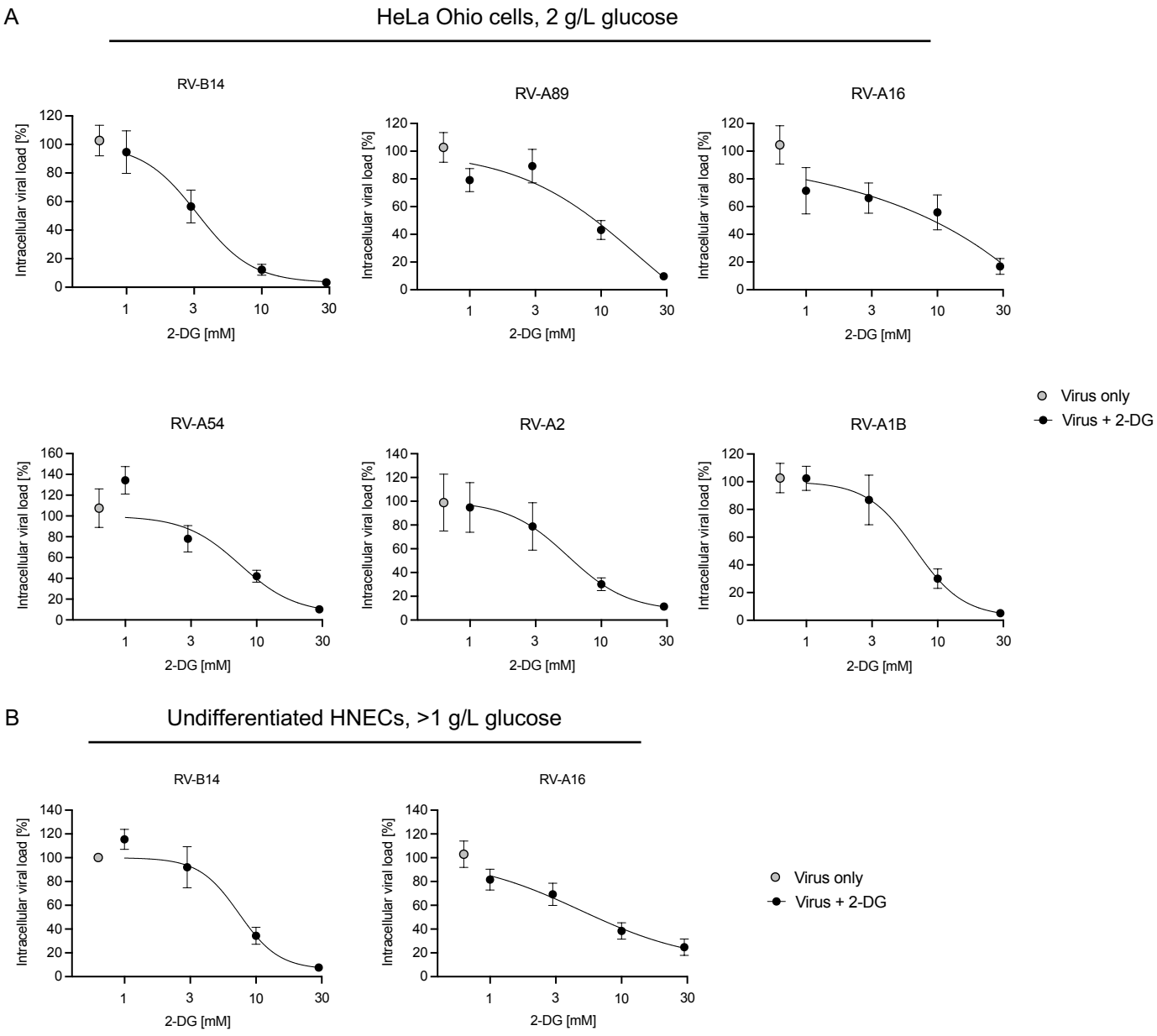

Figure 2

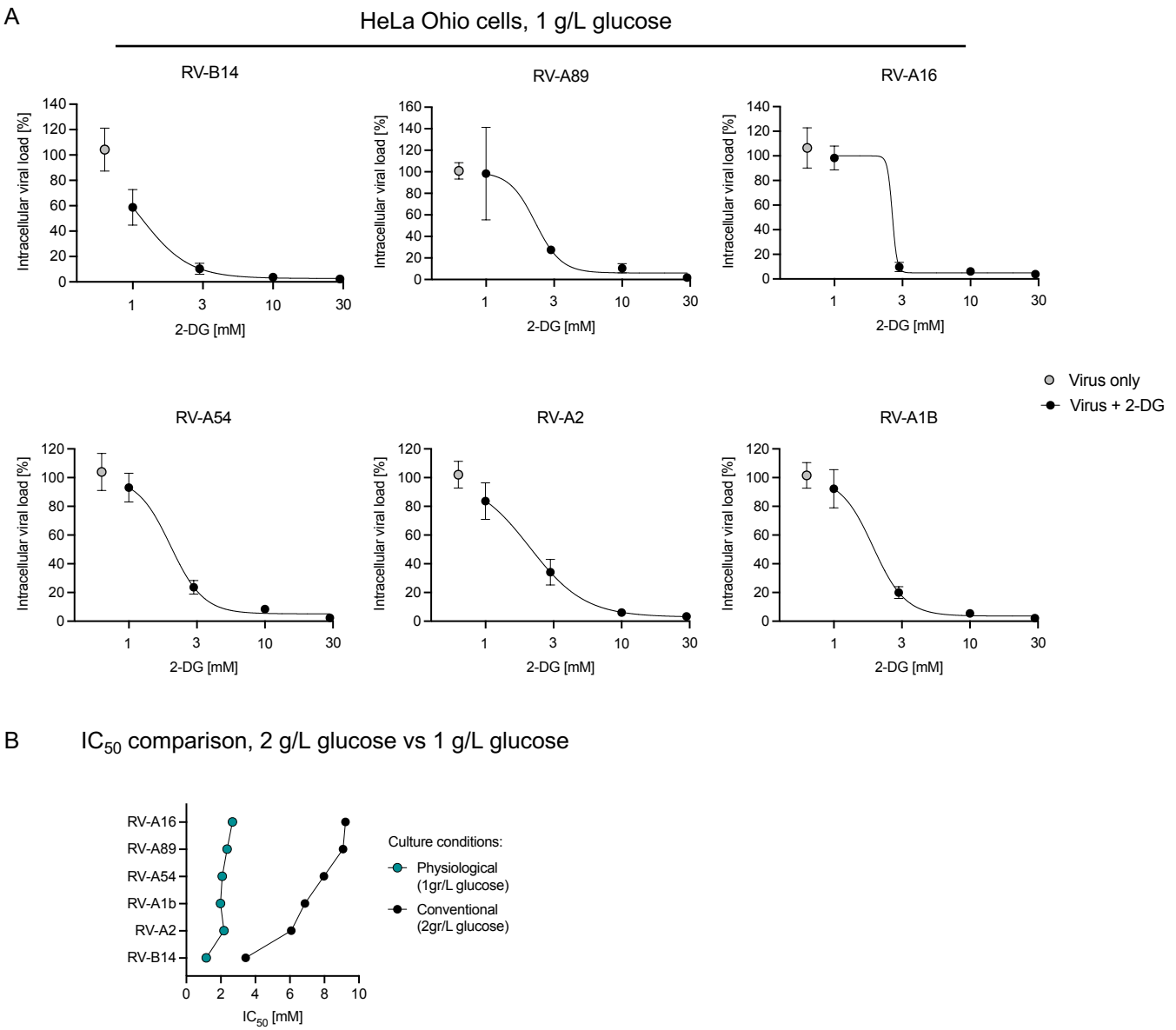

Figure 3

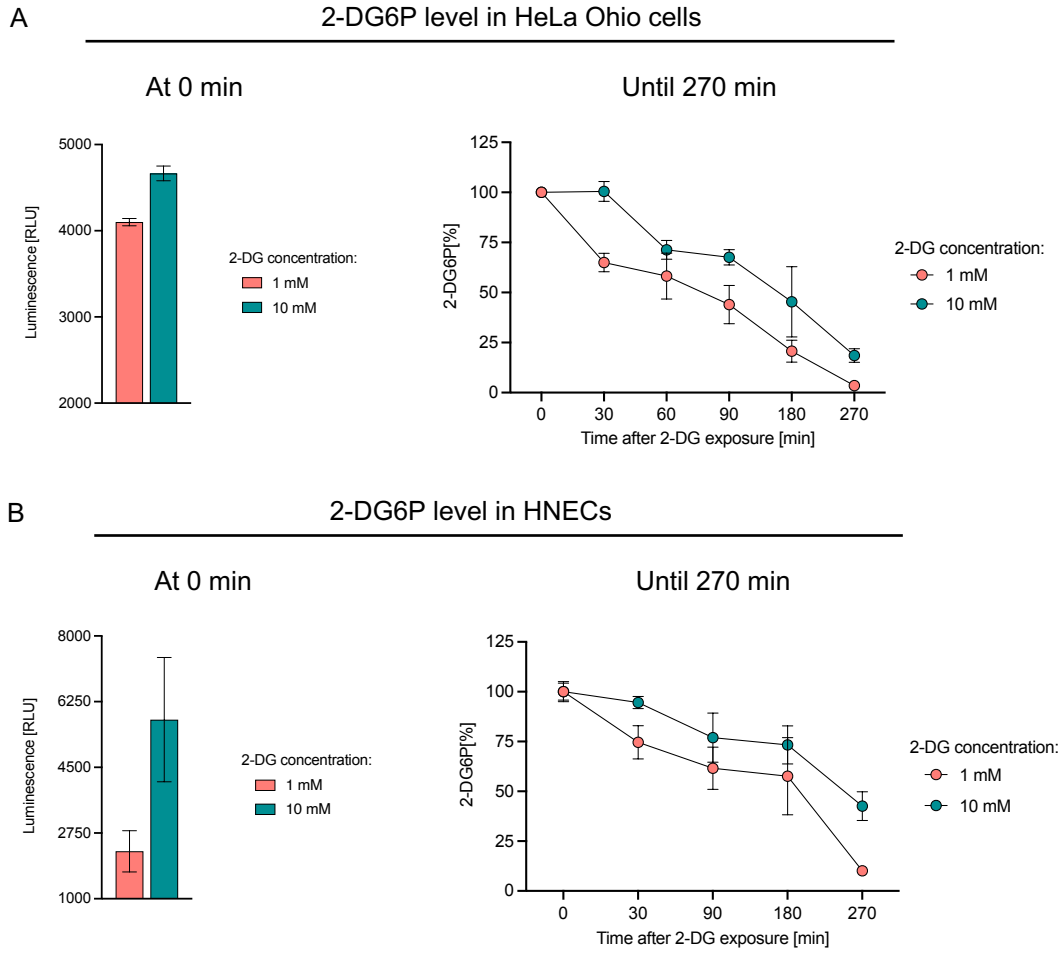

Figure 4

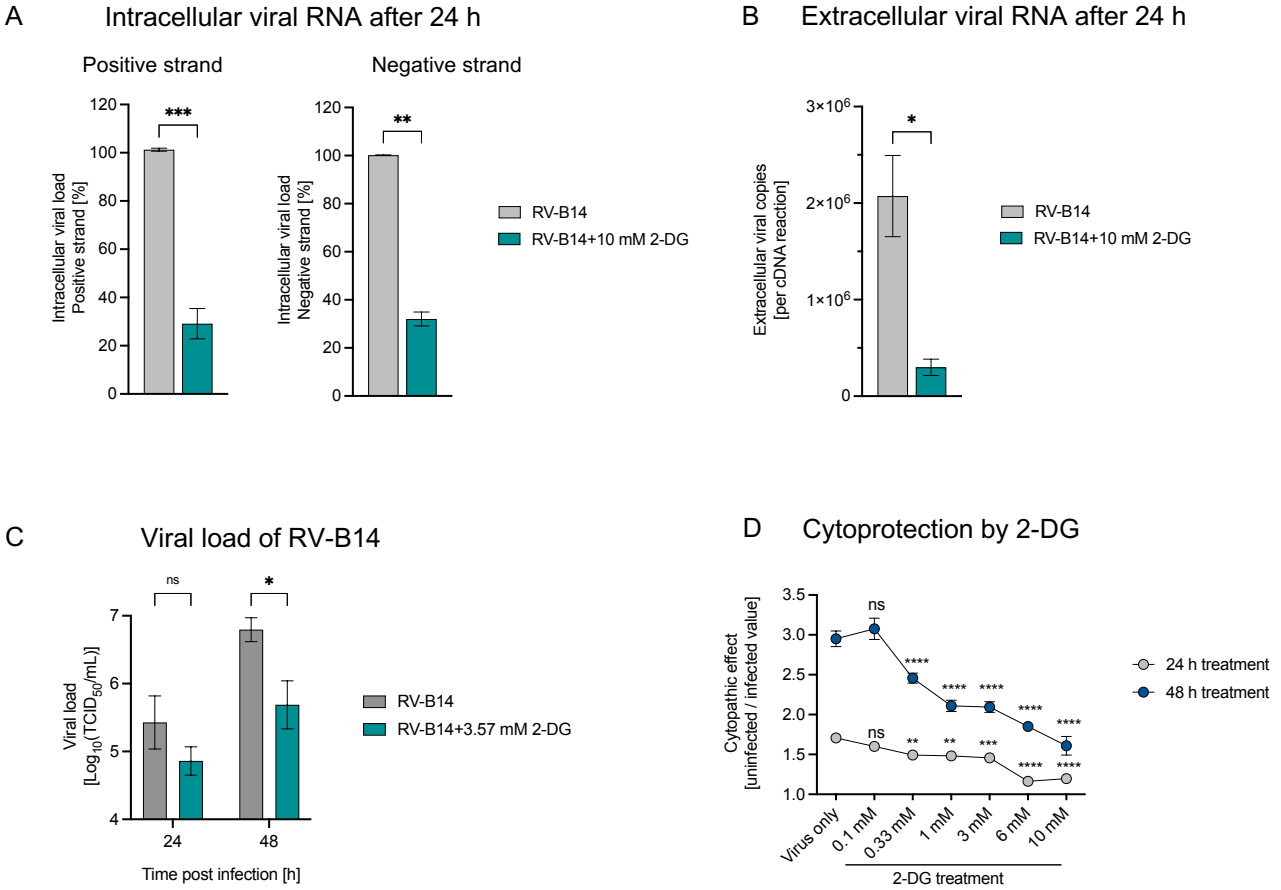

Figure 5